

## Multiboson production and polarisation measurements with the ATLAS detector

---

**Luka Selem\*** on behalf of the ATLAS Collaboration

*Univ. Grenoble Alpes, CNRS, LPSC-IN2P3  
38000 Grenoble, France*

*E-mail: [luka.selem@lpsc.in2p3.fr](mailto:luka.selem@lpsc.in2p3.fr)*

Measurements of multiboson production at the LHC are important probes of the electroweak gauge structure of the Standard Model and can constrain anomalous gauge boson couplings. Recent measurements of diboson and triboson production by the ATLAS experiment at  $\sqrt{s} = 13$  TeV and 13.6 TeV are presented. In triboson processes, the observations of the  $WZ\gamma$  and  $W\gamma\gamma$  channels are reported. In diboson processes, studies of gauge-boson polarisation and their correlation in  $WZ$  and for the first time in  $ZZ$  events are presented. In  $WZ$  events, these studies have been extended to phase space regions enriched with longitudinal polarisation and the Radiation Amplitude Zero effect is studied.

*31st International Workshop on Deep Inelastic Scattering (DIS2024)  
8–12 April 2024  
Grenoble, France*

---

\*Speaker

## 1. Introduction

The electroweak sector, with its non-abelian nature and its link to the Higgs mechanism, provides a number of sensitive probes of the Standard Model (SM). The study of processes producing two or three electroweak gauge bosons allows targeting triple and quartic gauge couplings which are as of yet still not well constrained. While triboson productions are very rare processes that start only now to be observed, diboson production is comparatively less rare allowing for more complex studies. One prime target is the study of the polarisation of both bosons produced with an emphasis on having both of them polarised longitudinally. This longitudinal degree of polarisation is only allowed for massive gauge bosons, the mass being itself a consequence of the Higgs mechanism. By the Goldstone equivalence theorem, at high energy, massive gauge bosons polarised longitudinally become equivalent to Goldstone bosons. As a result, studying longitudinal polarisation at high energy targets more precisely the Higgs mechanism. The ultimate goal is to study longitudinal vector boson scattering, a process with delicate cancellations in the Standard Model which ensure no cross section divergence at high energy.

This wide physics program is studied in proton–proton collisions at the LHC with the ATLAS experiment [1]. Recent results from ATLAS are presented here with the observations at  $\sqrt{s} = 13$  TeV of the triboson production processes  $WZ\gamma$  [2] and  $W\gamma\gamma$  [3] with  $140 \text{ fb}^{-1}$  of data. Polarisation measurements are reported with this dataset as well, in  $WZ$  production in special phase space regions enhancing longitudinal polarisation [4] and inclusively in  $ZZ$  production [5] for the first time. Finally, a measurement of the  $ZZ$  production cross section at  $\sqrt{s} = 13.6$  TeV with  $29 \text{ fb}^{-1}$  of data is reported [6], pioneering such electroweak measurements in LHC Run 3.

## 2. Triboson production

Triboson production are very rare processes, with cross sections several orders of magnitude below the total Higgs boson production. Historically, the first such process observed by both ATLAS and CMS in LHC Run 1 is the  $Z\gamma\gamma$  production, followed by  $\gamma\gamma\gamma$  in ATLAS. The Run 2 dataset provided observations of general triple massive bosons production  $VVV$  by CMS along more specific  $WWW$  production by ATLAS and  $WW\gamma$  by CMS. In the following, the first observations of the  $WZ\gamma$  [2] and  $W\gamma\gamma$  [3] processes by ATLAS are presented.

The  $WZ\gamma$  signature uses the leptonic (electron or muon) decay channel of both massive gauge bosons. It comprises a pair of same flavour opposite charged leptons with an invariant mass closest to the  $Z$  pole mass, one extra lepton and missing transverse energy for the  $W$  boson, and one isolated photon. A veto on a fourth lepton is used to reject  $ZZ\gamma$  production. Invariant mass selections and isolation criteria allow rejecting processes where the photon originates from a final state radiation. Non-prompt background is dealt with the data-driven *Fake Factor* method while irreducible  $ZZ$  and  $ZZ\gamma$  backgrounds are estimated with dedicated control regions. A profile-likelihood fit in the signal region and the two control regions allows observing  $WZ\gamma$  production with  $6.3 \sigma$  significance ( $5 \sigma$  expected). The cross section in the fiducial phase space is measured to be  $\sigma_{WZ\gamma}^{\text{Fid.}} = 2.01 \pm 0.30(\text{stat.}) \pm 0.16(\text{syst.}) \text{ fb}$ , consistent with the SM prediction within  $1.5 \sigma$ .

Comparatively, the  $W\gamma\gamma$  production has a higher cross section but is affected by a higher level of background. The event selection requires two high energy isolated photons, one isolated electron or

muon and missing transverse energy. A veto on a second lepton allows rejecting backgrounds with additional massive bosons. Requirements on the invariant mass and  $p_T$  of the lepton and photons allow rejecting the  $Z\gamma$  background. In the resulting signal region, the background still represents roughly half of the selected events. The main background processes, coming from non-prompt photons in jets, followed by electron misidentification as photon and non-prompt leptons in jets, are estimated with data-driven methods. Finally, a top control region, requiring one  $b$ -jet, is defined. A binned maximum likelihood fit in the signal and top control regions (Figure 1a) allows observing the  $W\gamma\gamma$  process with  $5.6\sigma$  significance ( $5.6\sigma$  expected). As demonstrated in Figure 1b, the cross section in the fiducial phase space agrees with the SM predictions. This measurement is dominated by systematic uncertainties related to the identification of prompt photons as a direct consequence of the importance of this type of background.

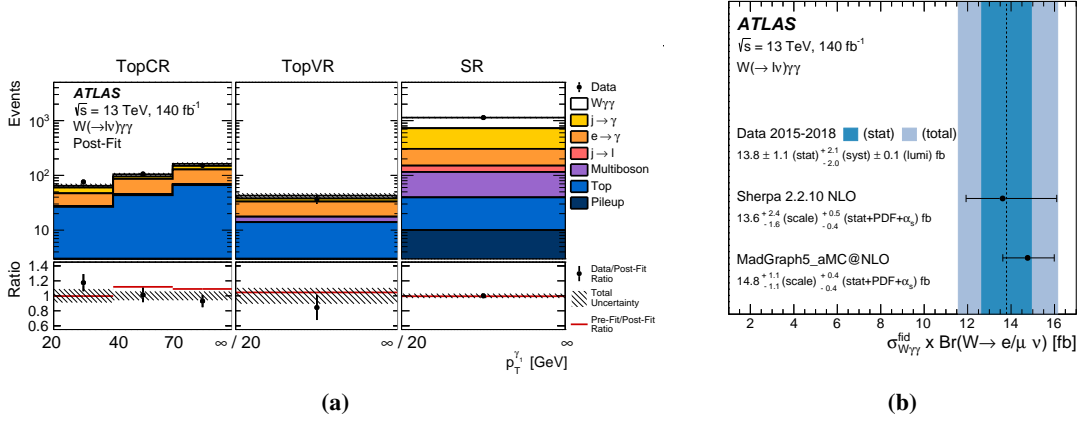


**Figure 1:** (a) Data, and pre- and post-fit yields for the top control region (TopCR) as a function of the leading photon  $p_T$ , and for the top validation region (TopVR) and signal region (SR) each as a single bin. (b) The measured fiducial  $W(\rightarrow e\nu/\mu\nu)\gamma\gamma$  cross section compared with signal event generator predictions. Both from [3].

### 3. $WZ$ polarisation measurement

The simultaneous extraction of both bosons polarisation in a diboson process was first performed in the  $WZ$  channel [7] which offers an experimental compromise between event yield and a clean signature. This ATLAS measurement reported for the first time an observation of the fully longitudinal joint-polarisation state with the measurement of the associated fraction  $f_{00}$ . To obtain such a result, pure joint-polarisation templates are used in a binned likelihood template fit of the distribution of a discriminating variable. The choice of this variable is key as with the limited event yield, a good discriminating power between all the joint-polarisation states is needed. Another key feature is the generation of these polarised templates at the highest order in perturbation theory available, as simple leading order (LO) templates are shown to bias the measurement. Additionally, the inclusive signal distribution is not directly the sum of the polarised templates, but can include an interference term which may not be negligible. Finally, it should be noted that for massive particles,

polarisation is not a Lorentz-invariant concept; the usual choice of the diboson system rest frame is made in the following.

In a recent study [4], the joint-polarisation measurement in the  $WZ$  channel was extended to phase space regions designed to enhance the longitudinal polarisation contribution. Two such regions are obtained with, on top of the usual  $WZ$  signal region selection [7], the additional  $p_T^Z \in [100, 200]$  GeV or  $p_T^Z > 200$  GeV selection. This allows probing the energy dependence of  $f_{00}$ . To reduce the contribution from next-to-leading order (NLO) effects, a  $p_T^{WZ} < 70$  GeV selection is applied as well. The output score of a Boosted Decision Tree (BDT) trained to discriminate the fully longitudinal state against all others is used as the template fit variable. The polarised templates are generated at LO with real NLO QCD corrections and their sum is reweighted to the inclusive NLO QCD prediction and scale-factors are derived from data in jet multiplicity bins of the inclusive selection. The contribution from interferences is found to be negligible. A binned likelihood template fit is performed, using the three unconstrained parameters  $f_{00}$ ,  $f_{0T+T0}$  (for the mixed joint-polarisation fraction) and the signal strength modifier, the remaining fully transverse fraction  $f_{TT}$  being extracted from the normalisation to one of the sum of fractions. The measured values of  $f_{00}$  in the longitudinally enhanced phase space regions, as reported in Table 1, are indeed higher than the value  $f_{00} = 0.067 \pm 0.010$  reported in the inclusive phase space [7]. All fractions values are in agreement with SM predictions.

	Measurement		Prediction	
	$100 < p_T^Z \leq 200$ GeV	$p_T^Z > 200$ GeV	$100 < p_T^Z \leq 200$ GeV	$p_T^Z > 200$ GeV
$f_{00}$	$0.19 \pm_{-0.03}^{+0.03}$ (stat) $\pm_{-0.02}^{+0.02}$ (syst)	$0.13 \pm_{-0.08}^{+0.09}$ (stat) $\pm_{-0.02}^{+0.02}$ (syst)	$f_{00}$ $0.152 \pm 0.006$	$0.234 \pm 0.007$
$f_{0T+T0}$	$0.18 \pm_{-0.08}^{+0.07}$ (stat) $\pm_{-0.06}^{+0.05}$ (syst)	$0.23 \pm_{-0.18}^{+0.17}$ (stat) $\pm_{-0.10}^{+0.06}$ (syst)	$f_{0T}$ $0.120 \pm 0.002$	$0.062 \pm 0.002$
$f_{TT}$	$0.63 \pm_{-0.05}^{+0.05}$ (stat) $\pm_{-0.04}^{+0.04}$ (syst)	$0.64 \pm_{-0.12}^{+0.12}$ (stat) $\pm_{-0.06}^{+0.06}$ (syst)	$f_{T0}$ $0.109 \pm 0.001$	$0.058 \pm 0.001$
$f_{00}$ obs (exp) sig.	$5.2$ (4.3) $\sigma$	$1.6$ (2.5) $\sigma$	$f_{TT}$ $0.619 \pm 0.007$	$0.646 \pm 0.008$

**Table 1:** Measured diboson joint-polarisation fractions in the two signal regions, along with the corresponding SM predictions. From [4].

Another striking feature of  $WZ$  production is the Radiation Amplitude Zero (RAZ) effect which predicts an exact cancellation of the fully transverse helicity amplitude when both bosons are produced orthogonally to the incoming quark direction. This results in a dip in the rapidity difference between the bosons at  $\Delta Y_{WZ} = 0$ . This feature first studied in  $W\gamma$  production is a direct consequence of the electroweak gauge structure. The effect is however diluted by NLO corrections. This latter issue is controlled in three phase space regions with an increasingly tight  $p_T^{WZ}$  selection down to below 20 GeV, the previously described  $p_T^Z$  selection being dropped here. The backgrounds, 00 and 0T+T0 joint-polarisation templates for  $|\Delta Y_{WZ}|$  normalised to the SM prediction are then subtracted from data to isolate the fully transverse joint-polarisation contribution. The  $|\Delta Y_{WZ}|$  distribution is then unfolded in the three fiducial phase spaces, as exemplified in Figure 2a, exhibiting as expected a dip at value 0. Its depth, computed from this figure as  $\mathcal{D} = 0.5 - 1^{st} \text{bin} / 2^{nd} \text{bin}$  (the  $2^{nd}$  bin being twice as large as the  $1^{st}$  one), is found to agree with SM predictions as shown in Figure 2b.

#### 4. ZZ polarisation measurement

The event yield in the  $ZZ$  production channel is lower than in  $WZ$ , making the joint-polarisation fraction measurement recently reported by ATLAS [5] more challenging. However, in this case

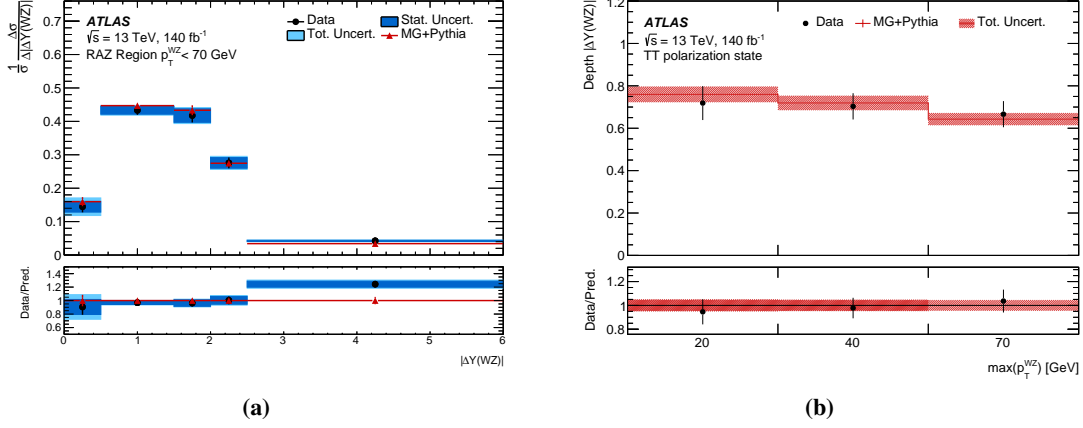


**Figure 2:** (a) Comparison between the 00+0T+T0-subtracted normalized unfolded  $|\Delta Y_{WZ}|$  data distribution and the theoretical prediction for TT events with  $p_T^{WZ} < 70$  GeV. (b) Depth of the RAZ dip for the unfolded  $|\Delta Y_{WZ}|$  distribution of the TT polarization as a function of the  $p_T^{WZ}$  selection value used. Both from [4].

the leptonic decay channel provides with precision the full kinematic information. The polar and azimuthal decay angle of both  $Z$  bosons and the production angle of the  $ZZ$  pair are used to train a BDT discriminating the fully longitudinal (LL) joint-polarisation state against the mixed (LT) and fully transverse (TT) ones<sup>1</sup>. The polarised samples are generated at LO with real NLO QCD corrections<sup>2</sup>. Then a theoretical fixed order NLO QCD+EW polarised template along the decay angle of a  $Z$  boson is used to reweight the polarised sample. An interference term found to have a sizeable impact is extracted reweighting the inclusive sample by the difference in the BDT distribution between the sum of the resulting polarised templates and the inclusive  $ZZ$  template. Finally, an inclusive reweighting of all samples is performed along two more variables. The impact of these NLO corrections on the templates can be seen in Figure 3a. Modelling uncertainties are derived doing the reweighting along an alternative variable and using the remaining non-closure of all samples.

A binned likelihood template fit of the BDT distribution (Figure 3b) manages to extract the LL contribution with  $4.3\sigma$  significance against the null hypothesis where there is no LL joint-polarisation state. This shows evidence for the fully longitudinal joint-polarisation state in  $ZZ$  production. The measurement is largely dominated by statistical errors, with a 23% relative uncertainty on  $\mu_{LL}$ , the normalisation parameter for the LL template. The leading systematic uncertainties arise from the modelling of the polarisation and interference templates. Finally, an optimal observable is built to search for Beyond the Standard Model (BSM) CP-odd anomalous neutral triple gauge couplings. It is designed to provide maximum sensitivity to these BSM models by combining  $Z$  boson polar and azimuthal decay angles. Its unfolded distribution in a fiducial phase space is in agreement with SM predictions allowing the setting of limits on these anomalous couplings.

<sup>1</sup>Note that in this paper, the longitudinal polarisation is noted "L".

<sup>2</sup>This applies for the dominant production mode  $q\bar{q} \rightarrow ZZ$ . The subdominant  $gg \rightarrow ZZ$  and Vector Boson Scattering productions mode are treated differently.

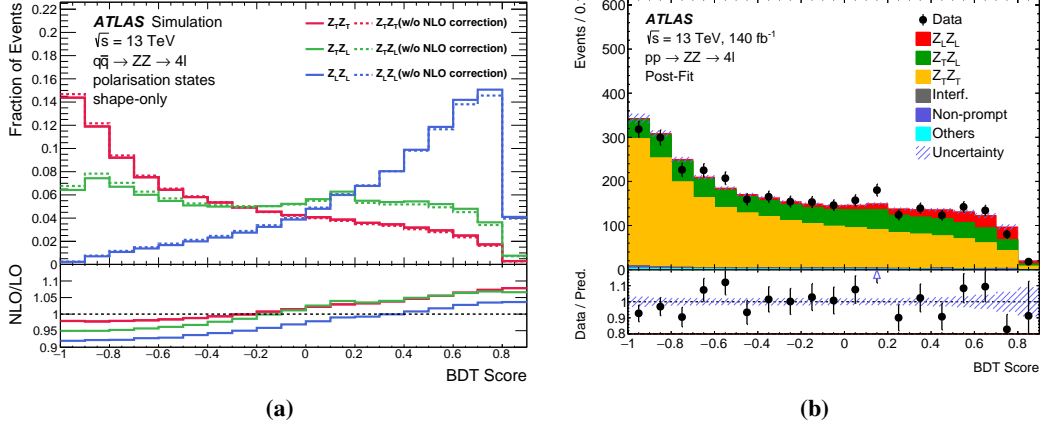


**Figure 3:** (a) BDT distributions normalised to the same area of the three polarisation templates, before (dashed lines) and after (solid lines) the reweighting procedure to account for higher-order corrections. (b) BDT distribution of data and post-fit SM predictions. The "Others" category represents the contribution from  $t\bar{t}Z$  and  $VVZ$ . Both from [5].

Finally, the inclusive  $ZZ$  analysis was redone using a  $29 \text{ fb}^{-1}$  dataset from LHC Run 3 [6]. It provides the first  $ZZ$  cross section at  $\sqrt{s} = 13.6 \text{ TeV}$  along with unfolded distributions, all in agreement with Standard Model. This work pioneers further diboson measurements in Run 3.

## 5. Conclusion

Multiboson processes and the particular aspect of their polarisations provide a variety of probes of the Higgs mechanism or the non-abelian structure of the electroweak theory. Two recent ATLAS triboson processes observation are reported:  $WZ\gamma$  and  $W\gamma\gamma$  with respectively  $6.3\sigma$  and  $5.6\sigma$  significances. In diboson processes, joint-polarisation fractions are measured in  $WZ$  and  $ZZ$  production. In  $WZ$  production, the evolution of the fully longitudinal state with energy is shown to agree with the SM prediction. The RAZ effect, a consequence of the gauge structure, is observed as well. In  $ZZ$  production, joint-polarisation fractions are measured for the first time showing evidence for the fully longitudinal state at  $4.3\sigma$  significance. These studies will now enter the Run 3 era, as exemplified by the early  $ZZ$  cross section measurement at  $\sqrt{s} = 13.6 \text{ TeV}$ .

## References

- [1] ATLAS Collaboration, *The ATLAS experiment at the CERN large hadron collider*, *Journal of Instrumentation* **3** (2008) S08003.
- [2] ATLAS collaboration, *Observation of  $WZ\gamma$  Production in  $pp$  Collisions at  $s=13 \text{ TeV}$  with the ATLAS Detector*, *Phys. Rev. Lett.* **132** (2024) 021802 [2305.16994].
- [3] ATLAS collaboration, *Observation of  $W\gamma\gamma$  triboson production in proton-proton collisions at  $\sqrt{s} = 13 \text{ TeV}$  with the ATLAS detector*, *Phys. Lett. B* **848** (2024) 138400 [2308.03041].

- [4] ATLAS collaboration, *Studies of the energy dependence of diboson polarization fractions and the Radiation Amplitude Zero effect in WZ production with the ATLAS detector*, [2402.16365](#).
- [5] ATLAS collaboration, *Evidence of pair production of longitudinally polarised vector bosons and study of CP properties in ZZ  $\rightarrow$  4 $\ell$  events with the ATLAS detector at  $\sqrt{s} = 13$  TeV*, *JHEP* **12** (2023) 107 [[2310.04350](#)].
- [6] ATLAS collaboration, *Measurement of ZZ production cross-sections in the four-lepton final state in pp collisions at s=13.6TeV with the ATLAS experiment*, *Phys. Lett. B* **855** (2024) 138764 [[2311.09715](#)].
- [7] ATLAS collaboration, *Observation of gauge boson joint-polarisation states in W $\pm$ Z production from pp collisions at s=13 TeV with the ATLAS detector*, *Phys. Lett. B* **843** (2023) 137895 [[2211.09435](#)].